Clinical Biomechanics 26 (2011) 955–961

Contents lists available at ScienceDirect

Clinical Biomechanics

journal homepage: www.elsevier.com/locate/clinbiomech

The effect of ankle foot orthosis stiffness on the energy cost of walking: A simulation study

D.J.J. Bregman [a,*], M.M. van der Krogt [a], V. de Groot [a], J. Harlaar [a], M. Wisse [b], S.H. Collins [b]

[a] MOVE Institute for Human Movement Research, Department of Rehabilitation Medicine, VU University Medical Center, Amsterdam, The Netherlands
[b] Delft University of Technology, Department of Biomechanical Engineering, Delft, The Netherlands

ARTICLE INFO

Article history:
Received 2 August 2010
Accepted 18 May 2011

Keywords:
Gait
Stroke
Multiple sclerosis
Biomechanics
Orthoses
AFO

ABSTRACT

Background: In stroke and multiple sclerosis patients, gait is frequently hampered by a reduced ability to push-off with the ankle caused by weakness of the plantar-flexor muscles. To enhance ankle push-off and to decrease the high energy cost of walking, spring-like carbon-composite Ankle Foot Orthoses are frequently prescribed. However, it is unknown what Ankle Foot Orthoses stiffness should be used to obtain the most efficient gait. The aim of this simulation study was to gain insights into the effect of variation in Ankle Foot Orthosis stiffness on the amount of energy stored in the Ankle Foot Orthosis and the energy cost of walking.
Methods: We developed a two-dimensional forward-dynamic walking model with a passive spring at the ankle representing the Ankle Foot Orthosis and two constant torques at the hip for propulsion. We varied Ankle Foot Orthosis stiffness while keeping speed and step length constant.
Findings: We found an optimal stiffness, at which the energy delivered at the hip joint was minimal. Energy cost decreased with increasing energy storage in the ankle foot orthosis, but the most efficient gait did not occur with maximal energy storage. With maximum storage, push-off occurred too late to reduce the impact of the contralateral leg with the floor. Maximum return prior to foot strike was also suboptimal, as push-off occurred too early and its effects were subsequently counteracted by gravity. The optimal Ankle Foot Orthosis stiffness resulted in significant push-off timed just prior to foot strike and led to greater ankle plantar-flexion velocity just before contralateral foot strike.
Interpretation: Our results suggest that patient energy cost might be reduced by the proper choice of Ankle Foot Orthosis stiffness.

© 2011 Elsevier Ltd. All rights reserved.

1. Introduction

In stroke and multiple sclerosis patients, gait is frequently hampered by a reduced ability to push-off with the ankle caused by weakness of the plantar-flexor muscles (Nadeau et al., 1999). A common strategy to compensate for this reduced ability to push-off is to deliver work around the hip joint (Lewis and Ferris, 2008; Nadeau et al., 1999). However, both physical experiments (Collins and Kuo, 2010) and modeling studies (Kuo, 2002; Ruina et al., 2005) indicate this is mechanically inefficient. This is due to the fact that work delivered at the hip fails to reduce the energy lost at foot strike, while ankle push-off does (Kuo, 2002). Parallel to a reduced ankle push-off, elevated energy cost of walking is observed in patients with stroke (Waters and Mulroy, 1999) and multiple sclerosis (Olgiati et al., 1988). This elevated energy cost might be explained by this mechanical inefficiency.

To enhance ankle push-off and to decrease the high energy cost of walking, carbon composite Ankle Foot Orthoses (AFOs) can be prescribed in patients with weakness of the plantar-flexor muscles (Bartonek et al., 2007; Desloovere et al., 2006; Wolf et al., 2008). This type of AFO functions like a spring; it stores energy starting from mid-stance and returns energy at the end of the stance phase (Bartonek et al., 2007; Desloovere et al., 2006; Wolf et al., 2008). It is expected that with more energy stored and released by the AFO, more functional benefit for the patient can be obtained (Bartonek et al., 2007; Desloovere et al., 2006; Wolf et al., 2008). This benefit could be expressed as a decrease in energy cost of walking (Brehm et al., 2008; Waters and Mulroy, 1999). Varying the rotational stiffness around the ankle may affect energy storage, push-off enhancement, and energy cost for the patient. However, the influence of AFO stiffness on energy cost, or the influence of other factors such as walking speed, has not been investigated.

In clinical practice, it is inconvenient to find the optimal AFO by testing a broad range of AFOs with different stiffnesses in each patient. Therefore, simulation models may be a useful alternative to explore the influence of AFO stiffness on the energy cost of walking. Complex simulation models with detailed representations of the leg muscles

* Corresponding author at: VU University Medical Center, Department of Rehabilitation Medicine, De Boelelaan 1117, 1081 HV Amsterdam, The Netherlands.
E-mail address: d.bregman@vumc.nl (D.J.J. Bregman).

0268-0033/$ – see front matter © 2011 Elsevier Ltd. All rights reserved.
doi:10.1016/j.clinbiomech.2011.05.007

have been used successfully to study pathological (Hicks et al., 2007; Van der Krogt et al., 2009) and normal gait (Anderson and Pandy, 2003). This type of model has also been used to predict neuromuscular adaptations that might be expected while using an AFO (Crabtree and Higginson, 2009). Another approach is to use "simple models," which are composed of coupled inverted pendulums that are powered by simple means such as gravity, springs, or constant torques (Hobbelen and Wisse, 2008; Kuo, 2002). By their simplicity, these models are suited to give insight in the basic mechanics of gait. Simple models have also been used successfully to obtain conceptual insights in pathological (Van der Krogt et al., 2010) and normal gait (Donelan et al., 2002b; Ruina et al., 2005). For example, models composed of coupled inverted pendulums have been used to study the effects of impulsive ankle push-off on the efficiency of gait (Kuo, 2002; Ruina et al., 2005), which led to the finding that the most efficient gait is achieved with impulsive ankle push-off just before contralateral heel strike.

In this study, we aim to gain insights in the conceptual mechanisms via which an AFO may influence pathological gait. To do so, we will use a simple dynamic model of gait to explore the role of the AFO. We will model the AFO as a passive linear spring (Bregman et al., 2009), and determine its influence throughout the gait cycle. As in patients (McNealy and Gard, 2008; Nadeau et al., 1999), the lack of active ankle push-off work will be compensated by work done at the hip joint.

The aim of this simulation study is to determine the effect of variation in AFO stiffness on energy cost of walking and the amount of energy stored in the AFO. At various walking speeds we will assess whether an optimal AFO stiffness is present in terms of minimal energy cost of walking, and whether this optimal stiffness coincides with the stiffness at which the most energy is stored in the AFO.

2. Methods

We developed a forward-dynamic, conceptual walking model with a passive spring at the ankle representing the AFO and two constant torques at the hip for propulsion. At seven walking speeds, we varied AFO stiffness while keeping walking speed and step frequency fixed. For each AFO stiffness we determined the amount of energy stored and returned by the AFO and the energy required to maintain steady gait (i.e. constant energy requirements and kinematics for consecutive walking cycles). Subsequently, the influence of walking speed was assessed by repeating this procedure at seven fixed walking speeds.

2.1. Model description

The two-dimensional 7-segment forward-dynamic model was developed analogous to previously developed models (Hobbelen and Wisse, 2008; Kuo, 2002; Van der Krogt et al., 2010). The model had 6 internal degrees of freedom, and was composed of an upper body, two upper legs, two lower legs and two feet (Fig. 1). The upper body, representing head, arms and torso, was modeled as a point mass located at the hip, neglecting the effects of arm swing and inertia of the torso. Leg segments and feet were modeled as rigid bodies. Length, mass, and inertial properties for the leg segments were based on average human anthropometry (Van Soest et al., 1993). The feet had anthropomorphic mass, but their rotational inertia was set to zero in order to avoid unwanted oscillations of the foot during the onset of swing. Table 1 lists the parameter values that were used in this study.

The joints between the segments were modeled as frictionless hinge joints. During stance, the knee joint of the stance leg was locked in full extension, implicitly assuming the leg to behave as an inverted pendulum rotating over the ankle joint (Cavagna et al., 1977). During swing, the knee joint was modeled as a frictionless hinge joint with a hyperextension stop. When full extension was reached an instantaneous inelastic collision occurred, after which the knee was kept locked in the extended position.

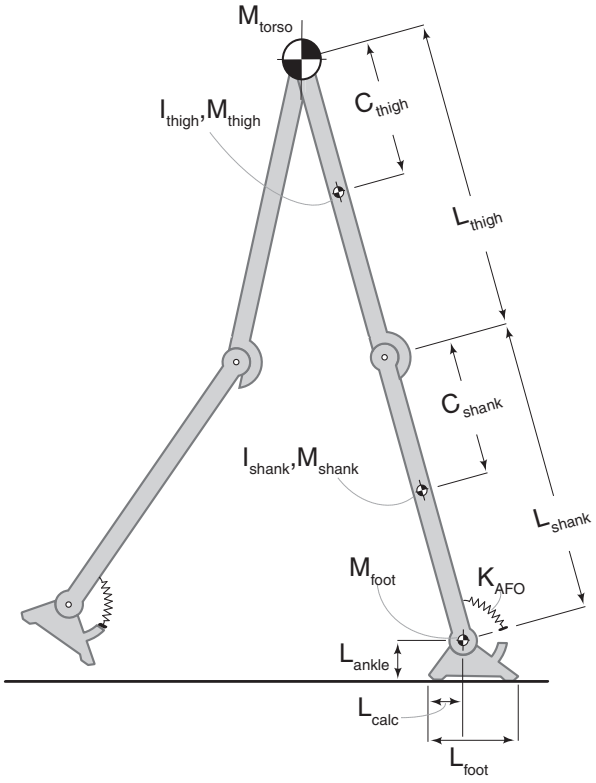

Fig. 1. Graphical representation of the two-dimensional, 7-segment model. Constant driving torques were applied to the stance and swing legs at the hip, reacting against a virtual torso.

The interactions between the model and the floor were modeled as rigid unilateral constraints, located in the heel and toe of the feet. The constraints were activated based on kinematic events (i.e. when the heel or toe touched the floor), at which point fully inelastic, instantaneous collision occurred (see Van der Krogt et al., 2010). The constraints were de-activated when the vertical forces between the contact points of the foot and the floor decreased to zero.

The AFO was modeled as a passive linear rotational spring acting on the ankle joint (Bregman et al., 2009). No other moments acted on the ankle joint, reflecting a completely paralyzed ankle. The AFO was applied bilaterally, modeling symmetric plantar-flexor weakness. The AFO was engaged when the ankle reached zero degrees of plantar-flexion during stance, so it was active during the portion of the gait cycle where most energy is stored and released in humans (Bartonek et al., 2007; Desloovere et al., 2006; Wolf et al., 2008). The model was powered at the hip, consistent with compensation strategies in patients with impaired push-off (McNealy and Gard, 2008; Nadeau et al., 1999). Energy input was provided by two constant hip torques acting solely on the upper legs. During swing, a flexion torque was applied onto the upper leg, and during stance an extension torque was

Table 1
Model anthropometry.

	Total	Upper body	Thigh	Shank	Foot
Mass m [kg]	82.25	55.77	8.47	3.53	1.24
Inertia I [kg l^2]		0	0.21	0.07	0
Length l [m]		0	0.485	0.458	0.16
Vertical CoM distance c [m]		0	0.21	0.198	0
Ankle height L_{ankle} [m]					0.06
Calcaneus depth $L_{calc.}$ [m]					0.04

The model parameters were based on human anthropometry of a male with a standing height of 1.86 m (Van Soest et al., 1993).

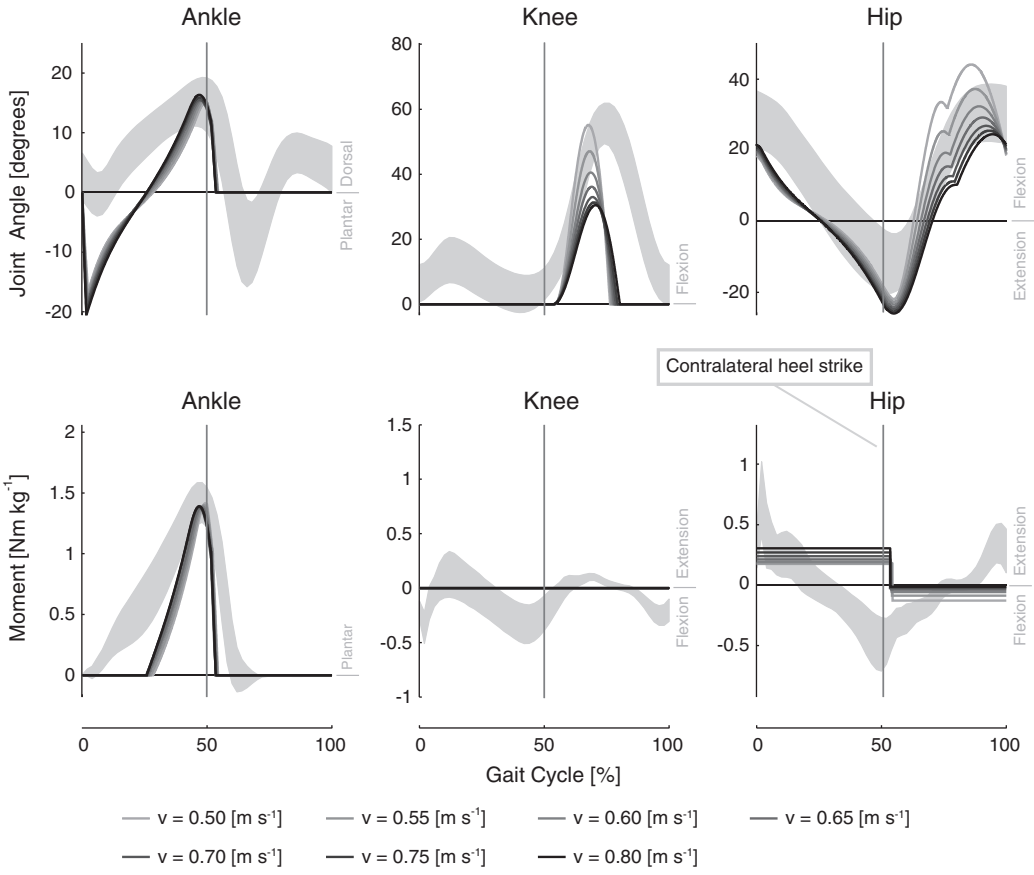

Fig. 2. Kinematics and kinetics produced by the model at walking speeds ranging from 0.50 to 0.80 m s^{-1}. The gray shading represent human reference data at 1.3 m s^{-1} (Winter, 1987). Because no moments are applied onto the knee, the knee joint moment is zero throughout the gait cycle.

applied onto the upper leg. These are simplified representations of hip torques that would react against a forward-leaning torso.

2.2. Simulation procedure

The equations of motion for the model were derived using a combination of the Newton–Euler and Lagrange methods known as the TMT method (Schwab and Wisse, 2001; Van der Krogt et al., 2010). Simulations were performed by solving the equations of motion forward in time in Matlab (The Mathworks, Natick, MA, USA). Each step was initiated with a set of initial orientations and velocities of the 7 segments, describing the state of the model. We searched for cyclic walking motions in which the state of the model at the initiation of a step was identical to the state after one complete step. A first-order gradient-search method was used to find cyclic walking motions, at which none of the orientations and velocities of the 7 segments changed more than $10e^{-5}$ over consecutive steps. We searched for cyclic walking motions for a broad range of AFO stiffnesses. To enable comparisons between different AFO stiffnesses, walking speed and step length were kept constant by adapting the magnitude of the hip flexion and extension torques. A higher-level first-order gradient search was used to find hip torques that resulted in the desired combination of speed and step length at each AFO stiffness. We enforced speeds and step lengths that followed a form similar to the relationship observed in humans (Grieve and Gear, 1966). To study the effect of walking speed, simulations over the range of AFO stiffnesses were performed at seven fixed walking speeds for which the model displayed cyclic walking behavior, ranging from 0.50 to 0.80 m s^{-1} with step frequency ranging from 0.82 step s^{-1} to 1.08 step s^{-1}.

2.3. Model outcome measures

For each simulated AFO stiffness, we calculated the amount of energy stored in the AFO and the energy cost of walking. To calculate the energy cost of walking, the amount of positive work done by the

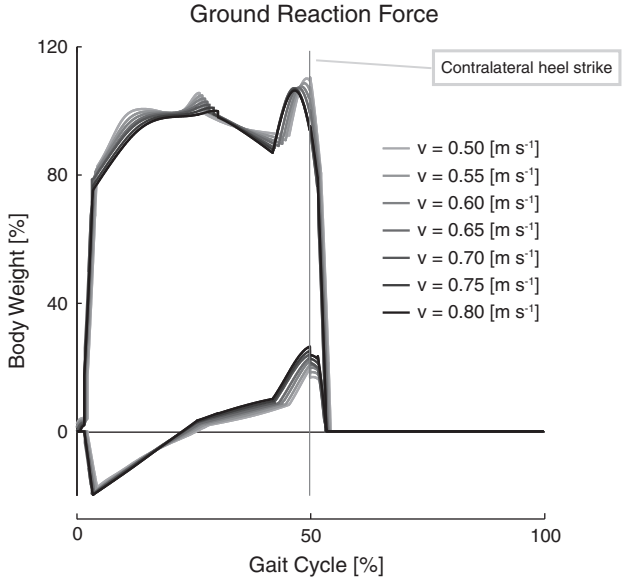

Fig. 3. Ground reaction force of a single leg at walking speeds ranging from 0.50 to 0.80 m s^{-1}.

two constant hip torques was summed. Subsequently, the amount of work per step was divided by the step length and mass of the model, giving energy cost of walking in J m^{-1} kg^{-1}. The amount of energy stored and returned by the AFO throughout the gait cycle was calculated as the integral of the moment exerted by the AFO onto the ankle over the ankle displacement. From this time series, the maximum amount of energy stored in the AFO, and the amount of preemptive push-off were obtained. The amount of preemptive push-off was defined as the amount of energy returned by the AFO before foot-flat (heel and toe in contact with the floor) of the contralateral leg. Furthermore, we calculated the ankle power by multiplying the ankle angular velocity and the moment exerted by the AFO.

3. Results

3.1. General model behavior

The model was able to walk for all imposed walking speeds ranging from 0.50 to 0.80 m s^{-1}. The model produced kinematics and kinetics (Fig. 2) and ground reaction forces (Fig. 3) comparable to human gait. The lowest AFO stiffness at which the model displayed walking behavior for the imposed walking speeds was 100 N m rad^{-1}. For high AFO stiffnesses (above 550 N m rad^{-1}), the model displayed oscillatory ankle behavior, which we chose not to consider. The model required between 0.27 and 0.90 J m^{-1} kg^{-1} to walk. The majority of this energy (40%–95%) was added to the system via the hip retroflexion torque. The energy losses in the model were predominantly (71%–86%) caused by the impact occurring at foot-flat. Minor energy losses were caused by the impact at heel strike and the impact at the knee extension stop.

3.2. Effect of AFO stiffness

3.2.1. Energy cost of walking

AFO stiffness strongly affected the energy cost of walking (Fig. 4). Results generated at a walking speed of 0.70 m s^{-1} showed a minimal energy cost of 0.27 J m^{-1} kg^{-1} at an AFO stiffness of 410 N m rad^{-1}. This optimal AFO stiffness resulted in an energy cost more than thee times lower than the energy cost with the lowest AFO stiffness. The highest AFO stiffness at which no ankle oscillations were observed was 550 N m rad^{-1}. At this stiffness the energy cost was 0.45 J m^{-1} kg^{-1}, almost twice the minimum energy cost.

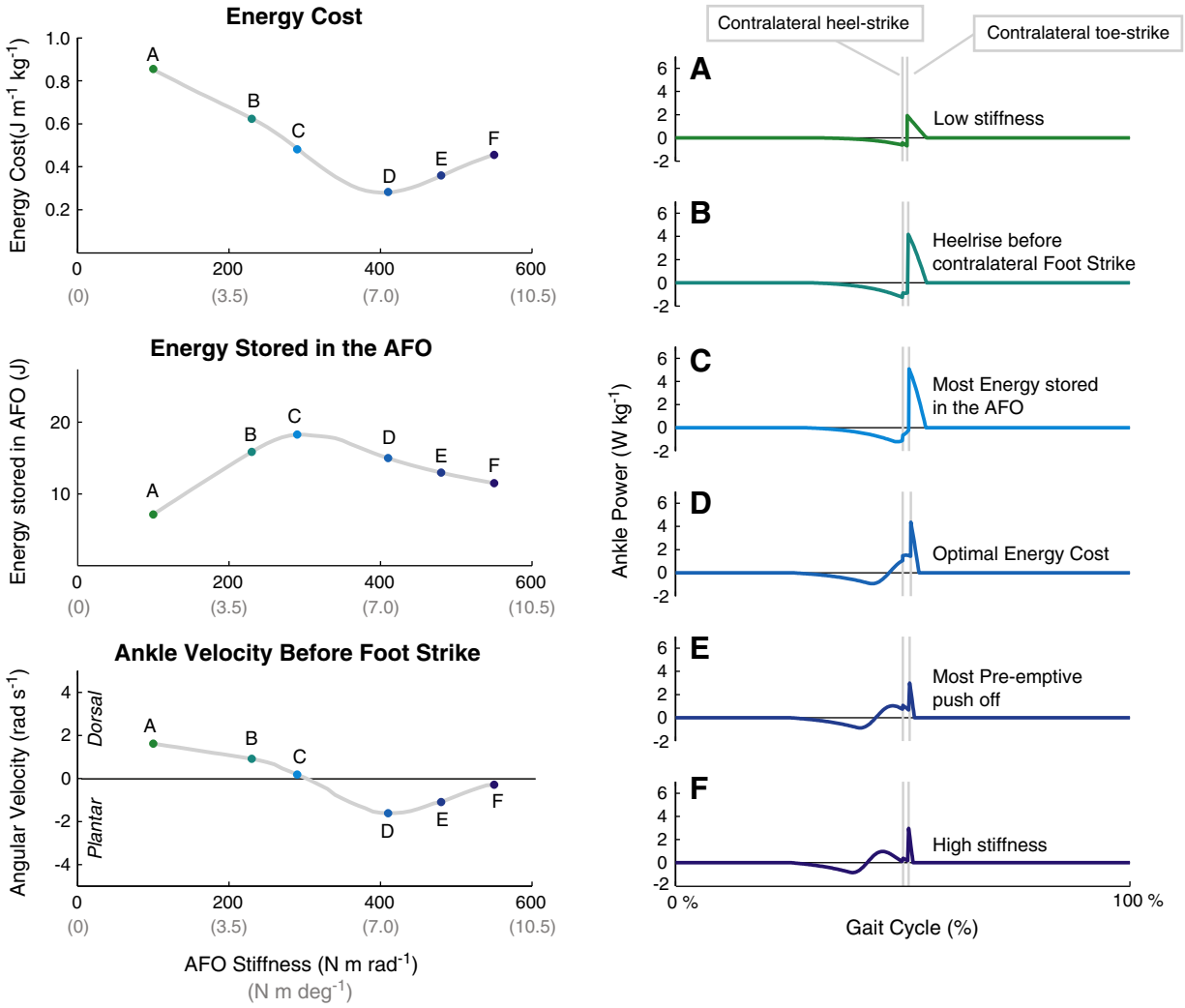

Fig. 4. *Left panels:* The effect of AFO stiffness on the energy cost of walking, on the amount of energy stored in the AFO, and on the ankle velocity before contralateral foot strike. *Right panels*: ankle power throughout the gait cycle displayed for typical stiffnesses (A–F), with corresponding outcomes indicated in the left panels. A: Low AFO stiffness, resulting in high energy cost, and low energy storage by the AFO. B: The lowest AFO stiffness for which heel rise occurs before contralateral heel strike. **C**: AFO stiffness at which the most energy is stored and released by the AFO. D: AFO stiffness resulting in the lowest energy cost of walking. E: AFO stiffness at which the most pre-emptive push-off occurs (i.e. most energy is returned by the AFO before contralateral foot strike). F: High AFO stiffness, with full energy return before contralateral foot strike. All results presented in this figure were generated at a walking speed of 0.70 m s^{-1}.

3.2.2. Energy stored in the AFO

The amount of energy stored in the AFO varied with the AFO stiffness distinctly (Fig. 4). At a walking speed of 0.70 m s^{-1}, a maximum of 18.3 J was stored at an AFO stiffness of 290 N m rad^{-1}. For higher and lower AFO stiffnesses, the amount of energy stored in the AFO was markedly lower. At the stiffness where the most energy was stored in the AFO, we found a sub-optimal energy cost of walking of 0.47 J m^{-1} kg^{-1}. Maximum preemptive push-off occurred at an AFO stiffness of 480 N m rad^{-1} and resulted in a sub-optimal energy cost of 0.35 J m^{-1} kg^{-1}.

3.2.3. Ankle angular velocity and center of mass velocity

The ankle angular velocity just before contralateral foot contact responded similarly to variations in AFO stiffness as the energy cost of walking (Fig. 4). For low AFO stiffnesses, the ankle had a dorsal-flexion velocity just before contralateral foot strike. For higher AFO stiffnesses the ankle had a plantar-flexion velocity, and thus returned energy before contralateral foot strike as can be seen from the corresponding ankle power curves (Fig. 4A–F). The highest plantar-flexion velocity at foot strike coincided with the optimal energy cost. With highest plantar-flexion velocity, the downward component of the center of mass velocity at foot strike was the smallest, and the least energy was lost as a result of the collision with the floor. At higher and lower stiffnesses, the ankle plantar-flexion velocity at foot strike was lower, the downward component of the center of mass velocity was larger, and more energy was lost as a result of the collision with the floor.

3.3. Walking speed

Optimal AFO stiffness was fairly constant over walking speeds ranging from 0.50 to 0.80 m s^{-1} (Fig. 5). The optimal AFO stiffness ranged from 420 N m rad^{-1} at a walking speed of 0.50 m s^{-1} to 390 N m rad^{-1} at a walking speed of 0.80 m s^{-1}. The optimal energy cost was 0.42 J m^{-1} kg^{-1} at 0.50 m s^{-1} and 0.32 J m^{-1} kg^{-1} at 0.80 m s^{-1}. At a walking speed of 0.65 m s^{-1} an overall minimal energy cost of 0.27 J m^{-1} kg^{-1} was found.

4. Discussion

The aim of this simulation study was to determine the effect of variations in AFO stiffness on AFO energy storage and return and the energy cost of walking at various walking speeds. In the forward-dynamic simulation model, we found an AFO stiffness that minimized the energy cost of walking. This optimal AFO stiffness did not coincide with the AFO stiffness at which the most energy was stored in the AFO, and was only slightly affected by walking speed.

The most efficient gait was found at the AFO stiffness where the AFO energy return redirected center of mass velocity upwards the most prior to contralateral foot strike. From previous studies it is known that the center of mass velocity before contralateral foot strike determines the amount of energy that is lost in the step-to-step transition (Kuo, 2002; Ruina et al., 2005). In our model the most efficient gait (i.e. with the least energy losses) was achieved with highest ankle plantar-flexion velocity just before contralateral foot strike, a kinematic indication that the center of mass velocity was most redirected upwards. Based on clinical practice, we expected that the most efficient gait would occur at the stiffness where most energy is stored and returned by the AFO. Yet in our model this stiffness was too low; it resulted in sub-optimal efficiency because the energy was not returned before contralateral foot strike and therefore not used to reduce the energy lost in the step-to-step transition. The stiffness where the most energy was returned before contralateral foot strike was too high; it resulted in a suboptimal energy cost because the redirection of the center of mass velocity by push-off was subsequently counteracted by gravity. As can be seen in Fig. 6, the negative

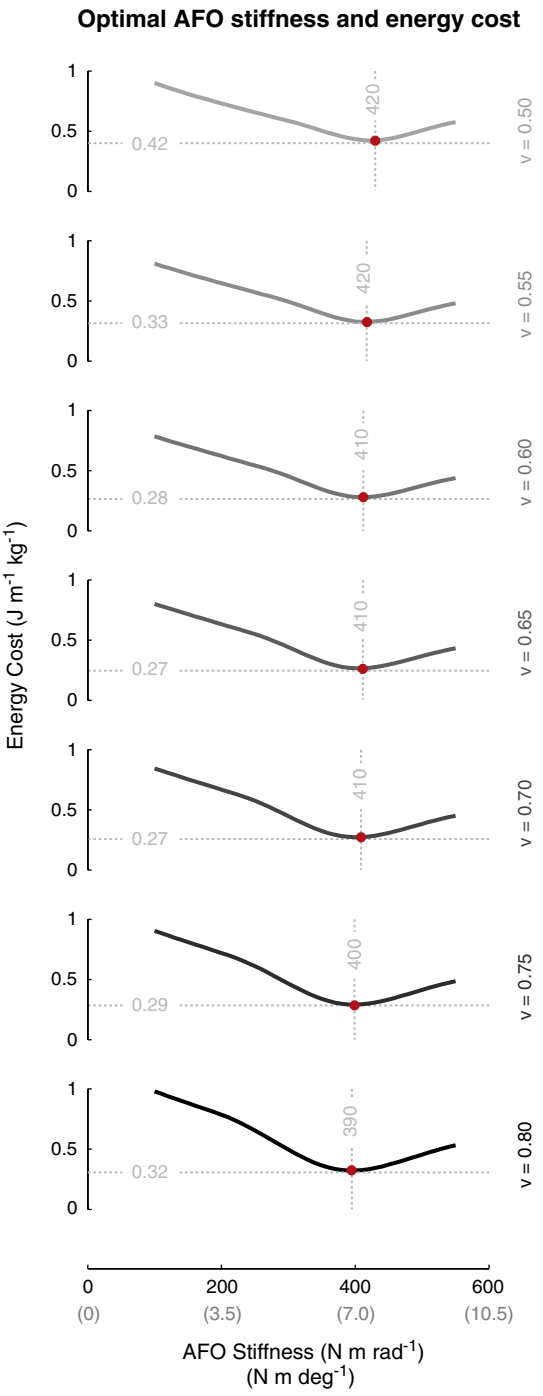

Fig. 5. The effect of walking speed on the energy cost of walking-AFO stiffness relationship, for walking speeds ranging from 0.50 to 0.80 m s^{-1}. The optimal AFO stiffness ranged from 420 N m^{-1} rad^{-1} at a walking speed of 0.50 m s^{-1} to 390 N m^{-1} rad^{-1} at a walking speed of 0.80 m s^{-1}.

impulse of the net vertical force acting on the center of mass results in a higher downwards velocity, which causes increased energy losses at contralateral foot strike. This refines predictions (Kuo, 2002; Ruina et al., 2005) that the most efficient gait is likely to be achieved with the most work before contralateral foot strike, and comports with the observation that the impulse of gravity significantly contributes to center of mass velocity changes during step-to-step transitions (Yeom and Park, 2011).

Our model produced walking behavior resembling human gait. The walking speeds produced by the model were similar to those

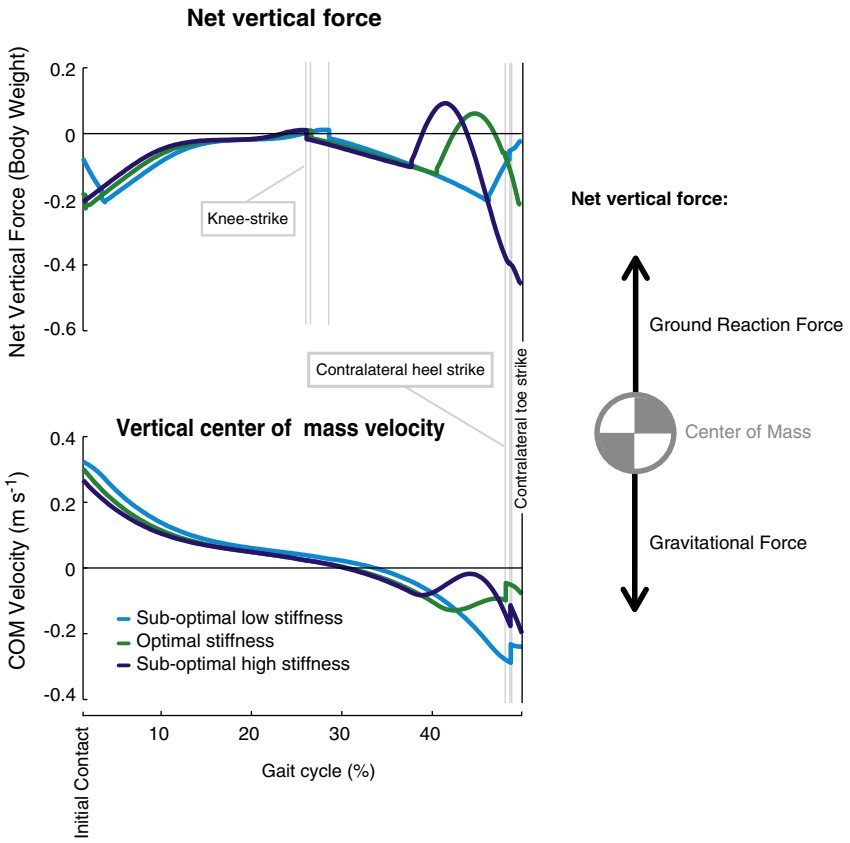

Fig. 6. Graphical explanation of the influence of gravity on the vertical center of mass velocity. The upper panel represents the net vertical force on the center of mass calculated as the sum of the gravitational force (F_g) and the vertical ground reaction force (GRF). A negative net vertical force indicates a downwards acceleration of the center of mass, as F_g>GRF. With sub-optimally low stiffness, push-off timing is too late, resulting in an absent upwards impulse before contralateral foot strike. At the optimal AFO stiffness, push-off timing results in a substantial positive upward impulse before contralateral foot strike. With sub-optimally high stiffness a positive upward impulse is also observed, however because push-off timing is too early, this is succeeded by a substantial gravity-induced downward impulse before contralateral foot strike. As can be seen in the lower panel, this results in a higher downward velocity of the center of mass, and thereby higher energy losses at contralateral foot strike. Discontinuities in this graph are the result of instantaneous gait events in the model, such as the locking of the knee at full extension. All results presented in this figure were generated at a walking speed of 0.70 m s^{-1}.

observed for stroke and multiple sclerosis patients (Perry et al., 1995). These speeds are slower than average normal gait (Winter, 1987), consistent with the absence of active ankle push-off (Hansen et al., 2004; McNealy and Gard, 2008). The kinematics and kinetics produced by the model were qualitatively similar to human gait (Fig. 2). The ankle showed more plantar-flexion in early stance, which may have originated from the absence of an ankle moment at this part of the gait phase. For simplicity, a constant hip torque was input to the model, which did consequently follow a different pattern than the human reference (Winter, 1987). Nonetheless, values were in the range of human walking (Winter, 1987). Moreover, similar hip extension moments throughout the stance phase have been observed in amputees wearing spring-like prostheses (Winter and Sienko, 1988). The ground reaction force produced by our model did not follow the characteristic M-wave (Fig. 3), which appears to be a direct consequence of the absence of a compliant knee in our model during stance (Geyer et al., 2006).

The energy cost of walking observed in our study was comparable to amount of negative external work during the step-to-step transition in human gait (0.20 to 0.40 J kg^{-1} m^{-1}) (Donelan et al., 2002a). In our model, work was delivered at the hip only, in order to overcome the energy lost in the step-to-step transition. The energy cost of walking observed in our study was substantially lower than the metabolic energy cost measured in healthy and pathological populations (Brehm et al., 2006), which may be due to the efficiency of the musculo-skeletal system and the fact that we used a frictionless planar model with only actuation at the hip. However, the external work and the metabolic energy cost are known to show great qualitative correspondence (Donelan et al., 2002b).

Our findings indicate that it is not only the amount of energy returned by the AFO, but also the timing of energy return by the AFO that determines the energy cost of walking. When the AFO is too compliant, energy cannot be used to reduce collision losses—push-off timing is too late. When the AFO is too stiff, push-off occurs too early, and the effects of push-off are diminished by the subsequent influence of gravity. The importance off push-off timing has also been noted in the clinical population. For example Brehm et al. (2008) reported that the timing of the peak push-off power in the ankle is an essential factor in the benefit of AFOs in Cerebral Palsy gait. In addition, it has been suggested that the AFO neutral angle (i.e. AFO alignment) is of influence on ankle kinetics (Miyazaki et al., 1997), and thereby on push-off timing. In our study we kept the AFO neutral angle constant, however it may be useful to study the role of the AFO neutral angle in the future.

In this study, we used a conceptual model of human walking that represents the complex human musculoskeletal system during gait. The use of this conceptual model allowed us to gain generic insights in how an AFO may affect pathological gait. The assumptions made by the choice of this model should be considered when interpreting our findings. The AFO stiffnesses applied in the model ranged from 100 to 550 N m rad^{-1}, with an optimal AFO stiffness of approximately 410 N m rad^{-1} (.087 N m deg^{-1} kg^{-1}). This stiffness resembles the quasi-stiffness of the ankle during normal gait (Frigo et al., 1996). However, the optimal AFO stiffness in our model is higher than the

average AFO stiffnesses reported in literature (Bregman et al., 2009; Stanhope et al., 2007), which might be the result of the absence of an active muscular system in our model. In order to translate our results to clinical practice, one must therefore assume the human ankle joint to have no stiffness or damping, which is adequate in the case of paralysis but not in presence of partially remaining ankle function, spasticity or contractures. Furthermore, we modeled the AFO bilaterally, whereas various pathologies require the AFO to be worn unilaterally. How the contralateral leg compensates for a reduced push-off while walking with a unilateral AFO could be investigated in future (modeling) studies, together with alternative strategies to compensate for a reduced ankle push-off.

Another simplification in our model is the role of the knee during energy return of the AFO. In our model, the energy of the AFO was returned with the knee in full extension. As a result, the energy returned by the AFO did not contribute to the swing leg as in normal gait (Meinders et al., 1998). With the introduction of an active knee joint, the cost of swinging the leg might therefore be lower at the hip. Adding a knee flexion torque to the model would have resulted in a substantial increase in complexity. However, it may be worth looking into the role of the knee torque and the contribution of the ankle push-off to leg swing in future studies.

Our findings emphasize the need to search for the optimal AFO stiffness for each patient in clinical practice, and suggest that a substantial improvement in the energy cost of walking may be achieved with the correct stiffness. Our findings contradict the intuitive idea that storing more energy in the AFO results in more efficient gait, and indicate that the timing of energy return by the AFO is an important factor that determines the energy cost of walking. The ankle plantarflexor velocity at contralateral heel strike may give a good indication of the adequacy of this timing. To test this in patients, future studies should not only focus on the effects of a typical type of AFO in a group of patients, but focus also on the influence of differences in AFO properties within individual patients.

Acknowledgements

The authors would like to thank Dr. Erwin van Wegen for providing his super-computer.

References

Anderson, F.C., Pandy, M.G., 2003. Individual muscle contributions to support in normal walking. Gait Posture 17, 159–169.
Bartonek, A., Eriksson, M., Gutierrez-Farewik, E.M., 2007. A new carbon fibre spring orthosis for children with plantarflexor weakness. Gait Posture 25, 652–656.
Bregman, D.J.J., Rozumalski, A., Koops, D., de Groot, V., Schwartz, M., Harlaar, J., 2009. A new method for evaluating ankle foot orthoses characteristics: BRUCE. Gait Posture 30, 144–149.
Brehm, M.A., Nollet, F., Harlaar, J., 2006. Energy demands of walking in persons with postpoliomyelitis syndrome: relationship with muscle strength and reproducibility. Arch. Phys. Med. Rehabil. 87, 136–140.
Brehm, M.A., Harlaar, J., Schwartz, M., 2008. Effect of ankle–foot orthoses on walking efficiency and gait in children with cerebral palsy. J. Rehabil. Med. 40, 529–534.
Cavagna, G.A., Heglund, N.C., Taylor, C.R., 1977. Mechanical work in terrestrial locomotion: two basic mechanisms for minimizing energy expenditure. Am. J. Physiol. 233, R243–R261.
Collins, S.H., Kuo, A.D., 2010. Recycling energy to restore impaired ankle function during human walking. Public Library of Science ONE.
Crabtree, C.A., Higginson, J.S., 2009. Modeling neuromuscular effects of ankle foot orthoses (AFOs) in computer simulations of gait. Gait Posture 29, 65–70.
Desloovere, K., Molenaers, G., Van, G.L., Huenaerts, C., Van, C.A., Callewaert, B., et al., 2006. How can push-off be preserved during use of an ankle foot orthosis in children with hemiplegia? A prospective controlled study. Gait Posture 24, 142–151.
Donelan, J.M., Kram, R., Kuo, A.D., 2002a. Simultaneous positive and negative external mechanical work in human walking. J. Biomech. 35, 117–124.
Donelan, J.M., Kram, R., Kuo, A.D., 2002b. Mechanical work for step-to-step transitions is a major determinant of the metabolic cost of human walking. J. Exp. Biol. 205, 3717–3727.
Frigo, C., Crenna, P., Jensen, L.M., 1996. Moment-angle relationship at lower limb joints during human walking at different velocities. J. Electromyogr. Kinesiol. 6, 177–190.
Geyer, H., Seyfarth, A., Blickhan, R., 2006. Compliant leg behaviour explains basic dynamics of walking and running. Proc. Biol. Sci. 273, 2861–2867.
Grieve, D.W., Gear, R.J., 1966. The relationships between length of stride, step frequency, time of swing and speed of walking for children and adults. Ergonomics 9, 379–399.
Hansen, A.H., Childress, D.S., Miff, S.C., Gard, S.A., Mesplay, K.P., 2004. The human ankle during walking: implications for design of biomimetic ankle prostheses. J. Biomech. 37, 1467–1474.
Hicks, J., Arnold, A., Anderson, F., Schwartz, M., Delp, S., 2007. The effect of excessive tibial torsion on the capacity of muscles to extend the hip and knee during single-limb stance. Gait Posture 26, 546–552.
Hobbelen, D.G.E., Wisse, M., 2008. Ankle actuation for limit cycle walkers. Int. J. Rob. Res. 27, 709–735.
Kuo, A.D., 2002. Energetics of actively powered locomotion using the simplest walking model. J. Biomech. Eng. 124, 113–120.
Lewis, C.L., Ferris, D.P., 2008. Walking with increased ankle pushoff decreases hip muscle moments. J. Biomech. 41, 2082–2089.
McNealy, L.L., Gard, S.A., 2008. Effect of prosthetic ankle units on the gait of persons with bilateral trans-femoral amputations. Prosthet. Orthot. Int. 32, 111–126.
Meinders, M., Gitter, A., Czerniecki, J.M., 1998. The role of ankle plantar flexor muscle work during walking. Scand. J. Rehabil. Med. 30, 39–46.
Miyazaki, S., Yamamoto, S., Kubota, T., 1997. Effect of ankle–foot orthosis on active ankle moment in patients with hemiparesis. Med. Biol. Eng. Comput. 35, 381–385.
Nadeau, S., Gravel, D., Arsenault, A.B., Bourbonnais, D., 1999. Plantarflexor weakness as a limiting factor of gait speed in stroke subjects and the compensating role of hip flexors. Clin. Biomech. 14, 125–135.
Olgiati, R., Burgunder, J.M., Mumenthaler, M., 1988. Increased energy cost of walking in multiple sclerosis: effect of spasticity, ataxia, and weakness. Arch. Phys. Med. Rehabil. 69, 846–849.
Perry, J., Garrett, M., Gronley, J.K., Mulroy, S.J., 1995. Classification of walking handicap in the stroke population. Stroke 26, 982–989.
Ruina, A., Bertram, J.E., Srinivasan, M., 2005. A collisional model of the energetic cost of support work qualitatively explains leg sequencing in walking and galloping, pseudo-elastic leg behavior in running and the walk-to-run transition. J. Theor. Biol. 237, 170–192.
Schwab, A.L., Wisse, M., 2001. Basin of Attraction of the Simplelest Walking Model. Proceedings of ASME Design Engineering Technical Conferences, Pittsburgh, Pennsylvania.
Stanhope, S.J., Siegel, K.L., Halstead, L.S., 2007. Contribution of dynamic ankle–foot orthoses to ankle moments during stance in gait. Proceedings of ISPO World Conference 2007 Vancouver, Canada.
Van der Krogt, M.M., Doorenbosch, C.A., Harlaar, J., 2009. The effect of walking speed on hamstrings length and lengthening velocity in children with spastic cerebral palsy. Gait Posture 29, 640–644.
Van der Krogt, M.M., Bregman, D.J.J., Wisse, M., Doorenbosch, C.A.M., Harlaar, J., Collins, S.H., 2010. How crouch gait can dynamically induce stiff-knee gait. Ann. Biomed. Eng. 38, 1593–1606.
Van Soest, A.J., Schwab, A.L., Bobbert, M.F., Van Ingen Schenau, G.J., 1993. The influence of the biarticularity of the gastrocnemius muscle on vertical-jumping achievement. J. Biomech. 26, 1–8.
Waters, R.L., Mulroy, S., 1999. The energy expenditure of normal and pathologic gait. Gait Posture 9, 207–231.
Winter, D.A., 1987. The biomechanics and motor control of human gait, 1st ed. University of Waterloo Press, Waterloo, Ontario, Canada.
Winter, D.A., Sienko, S.E., 1988. Biomechanics of below-knee amputee gait. J. Biomech. 21, 361–367.
Wolf, S.I., Alimusaj, M., Rettig, O., Doderlein, L., 2008. Dynamic assist by carbon fiber spring AFOs for patients with myelomeningocele. Gait Posture 28, 175–177.
Yeom, J., Park, S., 2011. A gravitational impulse model predicts collision impulse and mechanical work during a step-to-step transition. J. Biomech. 44 (1), 59–67.